

# Progressive Spatio-Temporal Bilinear Network with Monte Carlo Dropout for Landmark-based Facial Expression Recognition with Uncertainty Estimation

Negar Heidari and Alexandros Iosifidis

Department of Electrical and Computer Engineering, Aarhus University, Denmark  
{negar.heidari,ai}@ece.au.dk

**Abstract**—Deep neural networks have been widely used for feature learning in facial expression recognition systems. However, small datasets and large intra-class variability can lead to overfitting. In this paper, we propose a method which learns an optimized compact network topology for real-time facial expression recognition utilizing localized facial landmark features. Our method employs a spatio-temporal bilinear layer as backbone to capture the motion of facial landmarks during the execution of a facial expression effectively. Besides, it takes advantage of Monte Carlo Dropout to capture the model’s uncertainty which is of great importance to analyze and treat uncertain cases. The performance of our method is evaluated on three widely used datasets and it is comparable to that of video-based state-of-the-art methods while it has much less complexity.

## I. INTRODUCTION

Facial expression recognition (FER) has been widely studied in the past several years and it is of great importance in different areas of computer vision such as social robotics and human-computer interaction (HCI). Although deep learning models have a high ability in feature learning, there are different challenges for employing them in facial expression recognition. The intra-class variability, including variations in age, gender, pose, illumination, face scale and appearance, necessitates the use of complex deep learning models to extract the most useful features for expression recognition [1]. However, existing publicly available datasets are not large and diverse enough to train high-performing deep learning models. Thus, designing compact neural network architectures for real-time facial expression recognition that can achieve high performance is of great importance.

It has been shown that the FER performance can be improved by using localized facial landmarks [2]. The motion of facial landmarks during the execution of a facial expression effectively represents the dynamic motion of the most informative facial parts, such as eyes, nose and mouth, for facial expressions and it is also invariant to illumination conditions and face appearance. However, while it has been shown that multi-modal data fusion based on facial landmarks and images or videos can improve performance of image or video-based FER [3]–[5], deep learning models employing only facial landmark features have been rarely studied.

FER methods can be categorized in *static methods*, which use an image as input to classify the facial expression depicted in it, and *dynamic methods* which use videos or a sequence of

images as input to classify the facial expression by considering both spatial and temporal features for classification. In this work, we focus on dynamic facial expression recognition. Existing deep learning approaches for dynamic FER which utilize facial landmarks, typically concatenate their coordinates over multiple frames to form a sequence of vectors to be used by Recurrent Neural Networks (RNNs) [3], or reorganize them to form a grid map so that they can be in a form suitable to become the input of Convolutional Neural Networks (CNNs) [6]. Therefore, these methods are not capable to capture the dynamic spatial and temporal features encoded in the facial landmarks in a sequence of frames. Similar to human body skeletons which are used for human action recognition (HAR) [7], [8], facial landmarks are also non-Euclidean structured data that can be modeled by a graph in which the landmark points are the graph nodes and the relationships between them are the edges connecting graph nodes. Therefore, the Spatio-Temporal Graph Convolutional Networks (ST-GCNs) [7], [8], the Progressive ST-GCN (PST-GCN) [9] which tries to find an optimized ST-GCN architecture, or the recently introduced Spatio-Temporal Bilinear Network (ST-BLN) [10] can be employed to extract informative features from a sequence of graphs, encoding facial landmarks through different time steps, for facial expression recognition.

One aspect of a real FER system that is often neglected by FER methods is that of classification uncertainty. In a real-world scenario, the FER system will analyze the facial expressions of a person and take actions which can take the form of, for example, recommendations to perform an activity. Spurious misrecognized expressions caused either by misclassification due to a low-performing model, or by false identification of an expression (e.g. sadness instead of neutral) due to high uncertainty, would lead to frustration to the user. Thus, for a FER system to be practical, it needs to be based on a high-performing model which can run in real-time and estimate the uncertainty of its predictions.

In this paper, we propose the Progressive Spatio-Temporal Bilinear Network (PST-BLN) method for facial expression recognition. PST-BLN inherits the advantage of ST-BLN [10] to learn graph structures at each layer of the network topology without the requirement of a pre-defined graph structure, allowing for more flexible model design. Moreover, the PST-BLN method automatically defines an optimized, compact and

data-dependant network topology without the need of thorough experimentation using user-designed topologies. Moreover, we propose to capture the model’s uncertainty by training our PST-BLN model using Monte Carlo Dropout [11] for helping the users of FER system to treat uncertain cases explicitly.

## II. RELATED WORK

Facial landmarks have been widely used in FER methods in conjunction with other data modalities to enhance performance. Recently, many real-time facial landmark detection methods have been developed which achieve good performance in addition to their high efficiency [12].

Recently, a GCN-based method has been proposed in [13] which uses only facial landmarks for facial expression recognition. In [13], the landmark extractor [12] was adopted to extract accurate 2D coordinates of 68 landmark points from each facial image in an image sequence. The extracted landmarks were modeled by a directed spatio-temporal graph which is constructed using landmark points as nodes and triangle meshes among all landmarks, built by Delaunay method, as edges. Inspired by methods recently proposed for skeleton-based human action recognition, like the DGNN [14], the FER method [13] also employs a multi-layer spatio-temporal GCN model to extract features from the spatio-temporal facial landmark graph and introduces the extracted features to a fully connected classification layer to predict the facial expression.

## III. PROPOSED METHOD

This section describes the proposed PST-BLN method for dynamic landmark-based facial expression recognition. The description starts with the graph construction procedure, followed by the description of the Spatio-Temporal Bilinear Layer (ST-BLL) and the proposed PST-BLN method. The combination of PST-BLN with Monte Carlo Dropout for estimating the model’s uncertainty is finally described.

### A. Spatio-temporal graph construction

By extracting the facial landmarks of all the images in a sequence, a spatio-temporal graph  $\mathcal{G} = (\mathcal{V}, \mathcal{E})$  can be constructed where  $\mathcal{V}$  is the node set of 2D coordinates of the facial landmarks and  $\mathcal{E}$  is the set of graph edges encoding spatial and temporal connections between the landmarks through different time steps. In this work, we adopted the Dlib’s facial landmark extractor [15] to extract accurate 2D coordinates of 68 landmark points from each facial image. It has been shown in [13] that the landmarks of the outer region of the face do not contain informative features for different facial expressions. Therefore, we remove the first 17 facial landmarks of each image and keep only the 51 landmarks carrying features of the key facial parts for facial expression recognition. Facial landmarks in each graph are normalized by subtracting the central landmark (nose). The triangle meshes among all landmarks obtained by Delaunay method make the spatial graph edges. The central node (nose) is set as the master node which is connected to all other graph nodes.

The temporal graph edges connect each landmark into its corresponding landmark in its previous and subsequent frames.

We utilize the edge features of the graph which encode the motion of the facial muscles instead of the landmark coordinates. Each graph edge is bounded by two graph nodes and it can be defined as a feature vector representing both the length and direction information. As an example, we define the feature vector of a graph edge with source node  $v_i = (x_i, y_i)$  and target node  $v_j = (x_j, y_j)$  as  $e_{ij} = (x_i - x_j, y_i - y_j)$ . Therefore, each image in the sequence is modeled by a graph with  $E$  spatial edges and the PST-BLN receives as input a tensor  $\mathbf{X} \in \mathbb{R}^{F \times T \times E}$  encoding a sequence of  $T$  spatial graphs expressing the connections of the graph edges.  $F$  denotes the feature dimension of each edge feature  $e_{ij}$ .

### B. Spatio-Temporal Bilinear Layer

The ST-BLL is composed of a bilinear transformation and a temporal convolution. The bilinear transformation receives as input the representations for the  $E^{(l-1)}$  facial graph edges at layer  $l - 1$ , denoted by  $\mathbf{H}^{(l-1)}$ , and transforms them by using a learnable weight matrix  $\mathbf{W}^{(l)}$  as follows:

$$\mathbf{H}_s^{(l)} = \text{ReLU} \left( \mathbf{U}^{(l)} \mathbf{H}^{(l-1)} \mathbf{W}^{(l)} \right), \quad (1)$$

where  $\mathbf{U}^{(l)} \in \mathbb{R}^{E^{(l)} \times E^{(l-1)}}$  is a learnable matrix indicating the spatial weighted connections between the facial graph edges. This matrix is initialized randomly and it is optimized in an end-to-end manner jointly with the parameters of the entire network. Unlike GCN layers which use the graph Adjacency matrix in the spatial graph convolution, ST-BLL allows for freely deciding the dimensions of matrix  $\mathbf{U}$ . This means that ST-BLL allows for aggregating (or expanding) information of the graph edges leading to  $E^{(l)} < E^{(l-1)}$  (or  $E^{(l)} > E^{(l-1)}$ , respectively). In this paper, we chose to keep the number of graph edges constant for all ST-BLLs, and for notation simplicity we use  $E$  hereafter.

The spatially transformed feature tensor  $\mathbf{H}_s^{(l)} \in \mathbb{R}^{F^{(l)} \times T^{(l)} \times E}$  with  $F^{(l)}$  feature dimensions is introduced to the temporal convolution, which captures the motion of the facial muscles taking place in each facial expression by propagating the edge features of each spatial graph through the time domain using a standard 2D convolution with a predefined kernel size  $K \times 1$  aggregating edge features in  $K$  consecutive frames. The structure of the ST-BLL is shown in Fig. 1. Each layer of the network is equipped by two residual connections to stabilize the model by adding the input to the output of the bilinear mapping and the temporal convolution. The temporal convolution block is followed by batch normalization and ReLU activation function.

### C. Progressive spatio-temporal bilinear network (PST-BLN)

A ST-BLN model is composed of several ST-BLLs for feature extraction and one fully connected layer for classification. A network with  $l$  ST-BLLs, employs the global average pooling after the  $l^{\text{th}}$  layer to produce a feature vector of size  $F^{(l)} \times 1$ . The feature vector is introduced to a fully connected

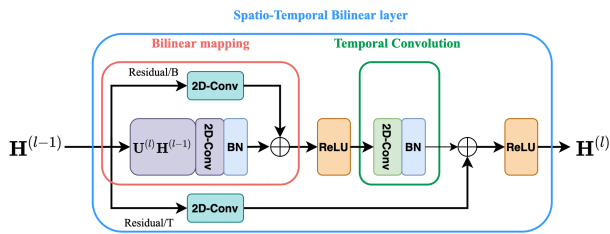


Fig. 1. Illustration of spatio-temporal bilinear layer  $l$ . It receives  $\mathbf{H}^{(l-1)}$  of size  $F^{(l-1)} \times T^{(l-1)} \times E$  as input and applies bilinear projection and temporal convolution to produce the output representation  $\mathbf{H}^{(l)}$  of size  $F^{(l)} \times T^{(l)} \times E$ . The bilinear mapping block and the temporal convolution block are both followed by batch-normalization (BN) and ReLU activation function.

layer which maps features from  $F^{(l)}$  to  $C$  dimensional subspace to classify features into  $C$  different classes.

Let us assume that a ST-BLN with  $l - 1$  layers has been already built, and the method proceeds in building the  $l^{th}$  layer. In practice, the bilinear projection and temporal convolution in 1 are standard 2D convolutions with filters of sizes  $F^{(l)} \times 1 \times 1$ , and  $F^{(l)} \times F^{(l)} \times K \times 1$ , respectively.  $F^{(l)}$  denotes the number of output channels in the  $l^{th}$  layer and  $K$  denotes the kernel size in the temporal convolution. The residual connections are also standard 2D convolutions which transform the input data of the layer with filters of size  $F^{(l)} \times 1 \times 1$  to have the same dimension as the layer's output. When the method starts building the  $l^{th}$  layer, the number of output channels in all the 2D convolutions is set to a predefined fixed number  $F^{(l)} = b$  and at each iteration, it is increased by  $F^{(l)} = F^{(l)} + b$ . While all the model's parameters in the previously built layers are initialized by the finetuned weights, the newly added neurons to the network are initialized randomly and all the model parameters are fine-tuned in an end-to-end manner using back-propagation. The layer's width progression at iteration  $t$  is evaluated according to the model's performance in terms of categorical loss value on training data, i.e.  $\alpha_w = (\mathcal{L}_{t-1}^{(l)} - \mathcal{L}_t^{(l)}) / \mathcal{L}_{t-1}^{(l)}$ .  $\mathcal{L}_{t-1}^{(l)}$  and  $\mathcal{L}_t^{(l)}$  denote the model's loss value at iterations  $t - 1$  and  $t$ , respectively. If  $\alpha_w < \epsilon_w$  with  $\epsilon_w > 0$ , it shows that increasing the layer's width doesn't improve the model's performance anymore and the method stops progression in that layer. Otherwise, the newly added parameters are saved and the next iteration starts increasing the layer's width by adding  $b$  more output channels to the filters of all the 2D convolutions in that layer.

This process repeats iteratively until the performance converges in that layer. After building each layer of the network, the method evaluates the model's depth progression using the rate of improvement in model's performance, i.e.  $\alpha_d = (\mathcal{L}^{(l-1)} - \mathcal{L}^{(l)}) / \mathcal{L}^{(l-1)}$ , in terms of categorical loss value on training data.  $\mathcal{L}^{(l-1)}$  and  $\mathcal{L}^{(l)}$  denote the model's loss value before and after adding the new layer to the network, respectively. When  $\alpha_d < \epsilon_d$  with  $\epsilon_d > 0$ , the method stops depth progression and the newly added layer is removed. Finally, all the model's parameters are fine-tuned together and the method returns the optimized topology for the ST-BLN model and its performance on training and validation data.

#### D. PST-BLN with Monte Carlo Dropout to model uncertainty

People of different ages, genders and cultural backgrounds have different levels of expressiveness, and they perform or interpret the facial expressions in different ways. Although the output of a classification model (softmax scores) encodes the predictive (pseudo-)probabilities of the model, it has been shown that even models with high softmax outputs can be uncertain about their predictions [16]. Since facial expression datasets are small in size, regularization of the network parameters is needed to prevent overfitting. To address this, we add a dropout layer after each ST-BLL built by the proposed method using a dropout rate  $p$  of 0.2. This choice also allows us to use Monte Carlo Dropout [16] to capture the uncertainty of the model during inference. This is very helpful for the users of the FER system to interpret the facial expression of a sample when the model is uncertain about its prediction. The main idea of Monte Carlo Dropout is to use dropout not only in the training phase, but also during the inference. Since dropout randomly switches off a subset of neurons in each layer, it can be interpreted as a Bayesian approximation of the Gaussian process. Every time the model provides classification result with activated dropout layers, its outputs are obtained from slightly different models with different sets of activated neurons and each of these models can be treated as a Monte Carlo sample. By repeating the inference for an input facial spatio-temporal graph with an activated dropout, the outputs of the PST-BLN are combined as an ensemble of different PST-BLN models and the variance in the outputs are used to capture the classification uncertainty.

## IV. EXPERIMENTAL RESULTS

### A. Datasets

The performance of our method has been evaluated on the following three widely used datasets:

**CK+** [17], [18]: The Extended Cohn-Kanade (CK+) contains 327 videos of 7 different emotional classes, starting from a neutral expression to peak expression. Similar to most methods using this dataset for evaluation, we select the first frame and the last three frames (including the peak expression) of each sequence for landmark extraction. Besides, the subjects are divided into 10 groups for 10-fold cross-validation.

**Oulu-CASIA** [19]: The Oulu-CASIA dataset consists of 2,880 image sequences of 80 subjects, captured under three different illumination conditions and using two different imaging systems; near-infrared (NIR) and visible light (VIS). We used the 480 image sequences captured by the VIS system under normal indoor illumination and we divided the subjects into 10 groups for 10-fold cross validation. In each image sequence, we used the last three frames, including the peak expression, and the first frame showing the neutral expression.

**AFEW** [20], [21]: The Acted Facial Expressions in the Wild (AFEW) dataset is a more challenging dataset for landmark extraction methods compared to the CK+ and Oulu-CASIA. It consists a set of video clips collected from movies with actively moving faces in different illumination and environ-

mental conditions. In some frames of each video where head pose is not frontal, the landmark extraction methods confront challenges to detect the face and extract its landmarks. Therefore, only a subset of video frames which provide meaningful facial landmark features are used. The dataset is divided into three sets, train, validation and test, with labels for the test set not being publicly available. Therefore, models are trained on the training set and evaluated on the validation set.

### B. Experimental setup

The experiments are conducted with GeForce RTX 2080 GPUs, SGD optimizer with weight decay of 0.0005 and momentum of 0.9 and cross entropy loss function. The models are trained on AFEW dataset for 300 epochs on 4 GPUs with learning rate of 0.01 and batch size of 64. For CK+ and Oulu-CASIA datasets, the models are trained for 400 epochs with learning rate of 0.1 and batch size of 128. The PST-BLN method is trained with block sizes of 5 and layer/block thresholds of 0.0001 for all three datasets.

Since AFEW dataset is challenging and it does not have sufficient amount of data for training the model, we adopted data augmentation to expand the dataset size by 14 times. First, for each video we extracted the landmarks from 150 frames which are sampled at same time intervals and when the number of frames with meaningful landmarks are less than 150, we repeat the frames by tiling method. After landmark extraction, similar to [3], [13], we added three different Gaussian noises to facial landmarks, then we applied random rotation to the noised data followed by random flipping to each sequence.

### C. Performance evaluation

The performance of the proposed method is compared with both video-based and landmark-based state-of-the-art methods on AFEW, Oulu-CASIA and CK+ datasets in Tables I, II, III, respectively. In each table, the state-of-the-art methods are divided into two groups. The first group contains the CNN-based or RNN-based methods which use videos or image sequences as the main data stream for training the model while some of these methods such as [22], [23] also utilize the landmark data in conjunction with video/image sequence to highlight the most important parts of the facial images and improve the performance. The second group contains the GCN-based methods which only use facial landmarks. To the best of our knowledge, the only GCN-based method that has been proposed for facial expression recognition is DGNN [13] which is an extension of [14] method for facial expression recognition. To show the effectiveness of our proposed model compared to other GCN-based networks, we also include in the comparisons the well-known GCN-based methods such as ST-GCN [7] and AGCN [8] to evaluate their performance on the landmark-based facial expression recognition task. Video-based methods train CNN and RNN-based architectures such as VGG16, LSTM, C3D, and they have the best performance on these datasets. However, the number of parameters of some of these methods is not reported in the corresponding papers.

TABLE I  
COMPARISON OF VIDEO/IMAGE-BASED AND LANDMARK-BASED METHODS ON THE VALIDATION SET OF AFEW DATASET

Method	Acc(%)	#Params	Data type
SSE-HoloNet [24]	46.48	-	Video
VGG-LSTM [25]	48.60	-	Video
C3D-LSTM [25]	43.20	-	Video
C3D-GRU [26]	49.87	-	Video
ST-GCN [7]	28.17	131.3k	Landmark
AGCN [8]	24.21	143.7k	Landmark
DGNN [14]	32.64	538k	Landmark
<b>ST-BLN w/MCD</b>	<b>36.11</b>	<b>132.3k</b>	Landmark
<b>ST-BLN wo/MCD</b>	34.13	132.3k	Landmark
<b>PST-BLN w/MCD</b>	<b>33.33</b>	<b>10.8k</b>	Landmark
<b>PST-BLN wo/MCD</b>	30.15	10.8k	Landmark

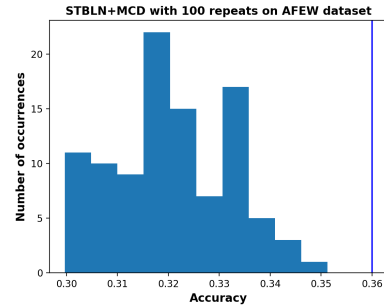


Fig. 2. The distribution of 100 classification accuracies obtained by the ST-BLN w/MCD method on AFEW dataset. The vertical line in the left side indicates the classification accuracy obtained by the ensemble predictions.

The ST-BLN model is composed of 7 ST-BLLs with output dimensions of  $\{8, 16, 16, 32, 32, 64, 64\}$ , respectively and a fully connected layer for classification. This model topology is the same as DGNN’s topology, and in order to have a fair comparison, we modified the topology of ST-GCN and AGCN models to have the same number of layers and layer dimensions as DGNN and ST-BLN models. While ST-GCN and AGCN methods utilize the landmark coordinates, or graph node features, and the squared Adjacency matrix of the graph in the spatial convolution, ST-BLN and PST-BLN utilize only the edge features of the graph. DGNN utilizes both node features and edge features encoded by a directed graph.

Experimental results on AFEW dataset indicate that ST-BLN outperforms all the baseline GCN-based methods, ST-GCN and AGCN, with a large margin while they have quite similar model complexity in terms of number of parameters. Compared to DGNN, ST-BLN has improved the classification performance by 4% while it has 4 times less number of parameters. PST-BLN which is trained with block sizes of 5 and layer/block thresholds of 0.0001, found an optimized topology for this dataset which is composed of 6 ST-BLLs with output sizes  $\{15, 10, 15, 5, 5, 10\}$ , respectively. This optimized model outperforms DGNN, ST-GCN and AGCN models with only 10.8k parameters which are 49 times less than those of DGNN.

To capture the model’s uncertainty, we evaluated both ST-BLN and PST-BLN models with activated dropout layers during the inference and we repeated the inference for 100

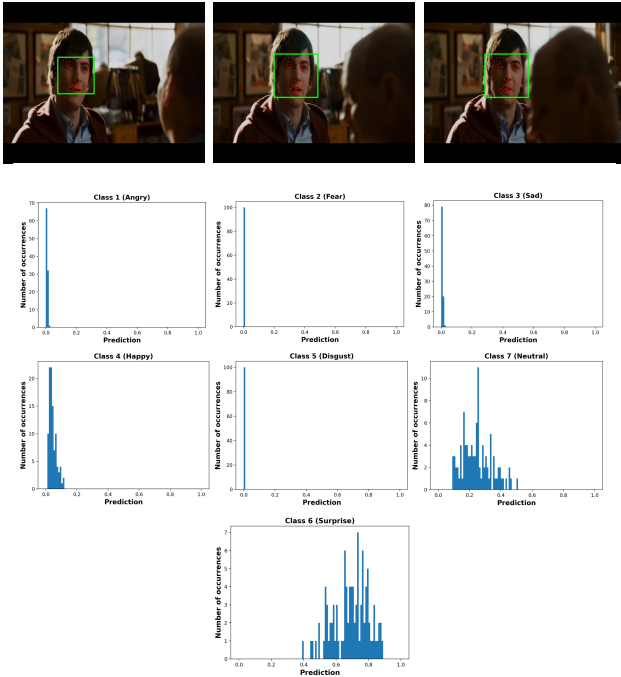


Fig. 3. Illustration of 3 frames of a sample video in AFEW dataset expressing ‘Surprise’, top row, and the distribution of 100 predictions for each class, obtained by our proposed ST-BLN model.

times on each sample to get 100 different prediction vectors. ST-BLN w/MCD and PST-BLN w/MCD denote the model’s classification accuracy obtained as the mean of 100 different predictions and ST-BLN wo/MCD and PST-BLN wo/MCD report the classification accuracy obtained by performing the inference only once. The results show that the model achieves better performance when it ensembles the predictions of 100 models rather than performing the inference only once. To calculate the model’s uncertainty on a dataset, we calculate the classification accuracy over 100 runs. Fig. 2, shows the distribution of 100 classification accuracy values of the ST-BLN w/MCD on AFEW dataset. The mean and standard deviation of this distribution are 32.09, 1.18, respectively. The classification accuracy obtained by the ensembled predictions is shown by a vertical line in the left side of the figure which is 36.11% and it is around 4% better than the mean accuracy.

Additionally, our proposed method gives the user the possibility of visualizing the model’s uncertainty on an individual sample base. As an example, we evaluated the ST-BLN model on a video sample of class Surprise from the AFEW dataset. Fig. 3 illustrates 3 frames of this video with their extracted facial landmarks and also the prediction distribution for each expression class. This figure shows that the model classifies this sample correctly in the Surprise class with mean probability of 0.69 while it is uncertain about it. Considering the sample frames in the top row of the figure, it can be seen that it is a hard example to classify and based on the prediction distributions, this example can also be classified in Neutral and Happy classes with mean probabilities of 0.24, 0.04, respectively. The variance of the model predictions of

TABLE II  
COMPARISON OF VIDEO-BASED AND LANDMARK-BASED METHODS ON OULU-CASIA DATASET USING 10-FOLD CROSS VALIDATION

Method	Acc(%)	#Params	Data type
DTAN [22]	74.38	-	Video
DTGN [22]	74.17	177.6k	Landmark
DTAGN [22]	81.46	-	Video + Landmark
PPDN [27]	84.59	6.8m	Video
PHRNN-MSCNN [23]	86.25	1.6m	Video + Landmark
DCPN [28]	86.23	-	Video
CDLM [29]	91.67	2.7m	Video
ST-GCN [7]	77.08	131.3k	Landmark
AGCN [8]	75.62	143.7k	Landmark
DGNN [14]	81.46	535,7k	Landmark
<b>ST-BLN w/MCD</b>	<b>83.54</b>	<b>132.3k</b>	Landmark
<b>ST-BLN wo/MCD</b>	<b>82.08</b>	<b>132.3k</b>	Landmark
<b>PST-BLN w/MCD</b>	<b>79.79</b>	<b>7.59k</b>	Landmark
<b>PST-BLN wo/MCD</b>	<b>78.74</b>	<b>7.59k</b>	Landmark

TABLE III  
COMPARISON OF THE VIDEO-BASED AND LANDMARK-BASED METHODS ON CK+ DATASET USING 10-FOLD CROSS VALIDATION

Method	Acc(%)	#Params	Data type
DTAN [22]	91.44	-	Video
DTGN [22]	92.35	177.6k	Landmark
DTAGN [22]	97.25	-	Video + Landmark
PPDN [27]	99.3	6.8m	Video
PHRNN-MSCNN [23]	98.5	1.6m	Video + Landmark
DCPN [28]	99.6	-	Video
CDLM [29]	98.47	2.7m	Video
ST-GCN [7]	93.64	131.3k	Landmark
AGCN [8]	94.18	143.7k	Landmark
DGNN [14]	96.02	535,7k	Landmark
<b>ST-BLN w/MCD</b>	<b>95.47</b>	<b>132.3k</b>	Landmark
<b>ST-BLN wo/MCD</b>	<b>93.19</b>	<b>132.3k</b>	Landmark
<b>PST-BLN w/MCD</b>	<b>93.34</b>	<b>9.79k</b>	Landmark
<b>PST-BLN wo/MCD</b>	<b>93.1</b>	<b>9.79k</b>	Landmark

each class can be interpreted as the model’s uncertainty on that class. Therefore, the model’s uncertainty on classes Surprise, Neutral and Happy is 0.1, 0.9, 0.02, respectively.

The mean classification performance of the models over all folds is reported for Oulu-CASIA and CK+ datasets. Since the PST-BLN method finds a different model topology for each fold of the data, we report the average number of parameters of 10 optimized models. Experimental results on Oulu-CASIA dataset show that the proposed ST-BLN model outperforms all the landmark-based methods while it has 4 times less number of parameters compared to the DGNN method. PST-BLN is trained separately for each of the 10 folds of the data and the average number of parameters is reported which is around 70 times less than DGNN and 17 times less than ST-BLN. Although the PST-BLN does not outperform the state-of-the-art methods, it is competitive while being much more compact.

ST-BLN outperforms the ST-GCN and AGCN on CK+ dataset while it has competitive performance compared to DGNN with around 4 times less number of parameters. The optimized topology PST-BLN achieves similar performance to the ST-GCN and AGCN with around 13 and 14 times less number of parameters. It should be noted that the reported number of parameters in all the tables corresponds only to the neural network models. As we use [15] for landmark detection, other methods such as [22], [23], [29] also utilize IntraFace [30] landmark extractor and [28] employs MTCNN [31] for face detection and alignment as a pre-processing step.

The results of ST-BLN w/MCD and PST-BLN w/MCD on Oulu-CASIA and CK+ datasets also confirm that repeating the inference with activated dropouts and ensembling the results, improves the classification performance.

## V. CONCLUSION

In this paper, we proposed a method which builds an optimized and compact spatio-temporal bilinear network topology for facial expression recognition by employing the localized facial landmarks instead of videos or image sequences. While our method has achieved comparable performance to more complex state-of-the-art methods, it captures the model's uncertainty using Monte Carlo Dropout technique which allows the user to analyze the model's prediction for different cases and take desired action.

## ACKNOWLEDGMENT

This work was supported by the European Union's Horizon 2020 Research and Innovation Action Program under Grant 871449 (OpenDR). This publication reflects the authors' views only. The European Commission is not responsible for any use that may be made of the information it contains.

## REFERENCES

- [1] Michel F Valstar, Marc Mehu, Bihan Jiang, Maja Pantic, and Klaus Scherer, "Meta-analysis of the first facial expression recognition challenge," *IEEE Transactions on Systems, Man, and Cybernetics, Part B (Cybernetics)*, vol. 42, no. 4, pp. 966–979, 2012.
- [2] Ali Mollahosseini, David Chan, and Mohammad H. Mahoor, "Going deeper in facial expression recognition using deep neural networks," in *IEEE Winter Conference on Applications of Computer Vision*, 2016.
- [3] Heechul Jung, Sihaeng Lee, Junho Yim, Sunjeong Park, and Junmo Kim, "Joint fine-tuning in deep neural networks for facial expression recognition," in *IEEE International Conference on Computer Vision*, 2015.
- [4] D. Kollias and S. P. Zafeiriou, "Exploiting multi-cnn features in cnn-rnn based dimensional emotion recognition on the omg in-the-wild dataset," *IEEE Transactions on Affective Computing*, pp. 1–1, 2020.
- [5] Behzad Hassani and Mohammad H. Mahoor, "Facial expression recognition using enhanced deep 3d convolutional neural networks," in *IEEE Conference on Computer Vision and Pattern Recognition Workshops*, 2017.
- [6] Jingwei Yan, Wenming Zheng, Zhen Cui, Chuangao Tang, Tong Zhang, and Yuan Zong, "Multi-cue fusion for emotion recognition in the wild," *Neurocomputing*, vol. 309, pp. 27–35, 2018.
- [7] Sijie Yan, Yuanjun Xiong, and Dahua Lin, "Spatial temporal graph convolutional networks for skeleton-based action recognition," in *AAAI Conference on Artificial Intelligence*, 2018.
- [8] Lei Shi, Yifan Zhang, Jian Cheng, and Hanqing Lu, "Two-stream adaptive graph convolutional networks for skeleton-based action recognition," in *IEEE Conference on Computer Vision and Pattern Recognition*, 2019.
- [9] Negar Heidari and Alexandros Iosifidis, "Progressive spatio-temporal graph convolutional network for skeleton-based human action recognition," in *IEEE International Conference on Acoustics, Speech and Signal Processing (ICASSP)*, 2021, pp. 3220–3224.
- [10] Negar Heidari and Alexandros Iosifidis, "On the spatial attention in spatio-temporal graph convolutional networks for skeleton-based human action recognition," *arXiv preprint arXiv:2011.03833*, 2020.
- [11] Joost van Amersfoort, Lewis Smith, Andrew Jesson, Oscar Key, and Yarin Gal, "Improving deterministic uncertainty estimation in deep learning for classification and regression," vol. abs/2102.11409, 2021.
- [12] Xuanyi Dong, Yan Yan, Wanli Ouyang, and Yi Yang, "Style aggregated network for facial landmark detection," in *IEEE Conference on Computer Vision and Pattern Recognition*, 2018.
- [13] Quang Tran Ngoc, Seunghyun Lee, and Byung Cheol Song, "Facial landmark-based emotion recognition via directed graph neural network," *Electronics*, vol. 9, no. 5, pp. 764, 2020.
- [14] Lei Shi, Yifan Zhang, Jian Cheng, and Hanqing Lu, "Skeleton-based action recognition with directed graph neural networks," in *IEEE Conference on Computer Vision and Pattern Recognition*, 2019.
- [15] Vahid Kazemi and Josephine Sullivan, "One millisecond face alignment with an ensemble of regression trees," in *IEEE Conference on Computer Vision and Pattern Recognition*, 2014.
- [16] Yarin Gal and Zoubin Ghahramani, "Dropout as a bayesian approximation: Representing model uncertainty in deep learning," in *International conference on machine learning*, 2016, pp. 1050–1059.
- [17] Patrick Lucey, Jeffrey F Cohn, Takeo Kanade, Jason Saragih, Zara Ambadar, and Iain Matthews, "The extended cohn-kanade dataset (ck+): A complete dataset for action unit and emotion-specified expression," in *IEEE Conference on Computer Vision and Pattern Recognition Workshops*, 2010.
- [18] Takeo Kanade, Jeffrey F Cohn, and Yingli Tian, "Comprehensive database for facial expression analysis," in *IEEE International Conference on Automatic Face and Gesture Recognition*. IEEE, 2000, pp. 46–53.
- [19] Guoying Zhao, Xiaohua Huang, Matti Taini, Stan Z Li, and Matti Pietikäinen, "Facial expression recognition from near-infrared videos," *Image and Vision Computing*, vol. 29, no. 9, pp. 607–619, 2011.
- [20] Abhinav Dhall, Roland Goecke, Simon Lucey, and Tom Gedeon, "Collecting large, richly annotated facial-expression databases from movies," *IEEE Annals of the History of Computing*, vol. 19, no. 03, pp. 34–41, 2012.
- [21] Abhinav Dhall, Roland Goecke, Jyoti Joshi, Karan Sikka, and Tom Gedeon, "Emotion recognition in the wild challenge 2014: Baseline, data and protocol," in *International conference on multimodal interaction*, 2014, pp. 461–466.
- [22] Heechul Jung, Sihaeng Lee, Junho Yim, Sunjeong Park, and Junmo Kim, "Joint fine-tuning in deep neural networks for facial expression recognition," in *IEEE International Conference on Computer Vision*, 2015.
- [23] Kaihao Zhang, Yongzhen Huang, Yong Du, and Liang Wang, "Facial expression recognition based on deep evolutionary spatial-temporal networks," *IEEE Transactions on Image Processing*, vol. 26, no. 9, pp. 4193–4203, 2017.
- [24] Ping Hu, Dongqi Cai, Shandong Wang, Anbang Yao, and Yurong Chen, "Learning supervised scoring ensemble for emotion recognition in the wild," in *ACM International Conference on Multimodal Interaction*, 2017.
- [25] Valentin Vielzeuf, Stéphane Pateux, and Frédéric Jurie, "Temporal multimodal fusion for video emotion classification in the wild," in *ACM International Conference on Multimodal Interaction*, 2017.
- [26] Min Kyu Lee, Dong Yoon Choi, Dae Ha Kim, and Byung Cheol Song, "Visual scene-aware hybrid neural network architecture for video-based facial expression recognition," in *IEEE International Conference on Automatic Face & Gesture Recognition*, 2019.
- [27] Xiangyun Zhao, Xiaodan Liang, Luoqi Liu, Teng Li, Yugang Han, Nuno Vasconcelos, and Shuicheng Yan, "Peak-piloted deep network for facial expression recognition," in *European Conference on Computer Vision*, 2016.
- [28] Zhenbo Yu, Qinshan Liu, and Guangcan Liu, "Deeper cascaded peak-piloted network for weak expression recognition," *The Visual Computer*, vol. 34, no. 12, pp. 1691–1699, 2018.
- [29] Chieh-Ming Kuo, Shang-Hong Lai, and Michel Sarkis, "A compact deep learning model for robust facial expression recognition," in *IEEE Conference on Computer Vision and Pattern Recognition Workshops*, 2018.
- [30] Xuehan Xiong and Fernando De la Torre, "Supervised descent method and its applications to face alignment," in *IEEE Conference on Computer Vision and Pattern Recognition*, 2013.
- [31] Kaipeng Zhang, Zhanpeng Zhang, Zhifeng Li, and Yu Qiao, "Joint face detection and alignment using multitask cascaded convolutional networks," *IEEE Signal Processing Letters*, vol. 23, no. 10, pp. 1499–1503, 2016.